Molecular Crystals and Liquid Crystals

Publication details, including instructions for authors and subscription information:
http://www.tandfonline.com/loi/gmcl20

Universal Mean-Field Phase Diagram for Biaxial Nematics

Fulvio Bisi [a]

[a] Dipartimento di Matematica and CNISM, Università di Pavia, Pavia, Italy

Version of record first published: 22 Sep 2010

To cite this article: Fulvio Bisi (2008): Universal Mean-Field Phase Diagram for Biaxial Nematics, Molecular Crystals and Liquid Crystals, 480:1, 182-201

To link to this article: http://dx.doi.org/10.1080/15421400701826316

Mol. Cryst. Liq. Cryst., Vol. 480, pp. 182–201, 2008

ISSN: 1542-1406 print/1563-5287 online
DOI: 10.1080/15421400701826316

Taylor & Francis
Taylor & Francis Group

Universal Mean-Field Phase Diagram for Biaxial Nematics

Fulvio Bisi
Dipartimento di Matematica and CNISM, Università di Pavia,
Pavia, Italy

Fully attractive and partly repulsive molecular interactions, characteristic of biaxial liquid crystal molecules, are described by a class of quadratic Hamiltonians, originally put forward by Straley. The partly repulsive interactions require a minimax principle for the associated mean-field free energy. By analyzing the different phases in a bifurcation scenario, we show that the phase diagram described by Sonnet et al. [Phys. Rev. E **67** *061701 (2003)] is universal. Our model predictions are in agreement with recent observations on both V-shaped and tetrapodal molecules.*

Keywords: biaxial; minimax principle; nematic liquid crystal

1. INTRODUCTION

The possibility that biaxial nematogenic molecules give rise to biaxial phases was already conceived in the 70's [1,2]. The quest for an experimental confirmation of biaxial nematic phases has had a long history since their existence was predicted theoretically. Although such quest has not yet ended, recently some researchers have claimed having successfully synthetized new nematogenic molecules that give rise to thermotropic biaxial phases [3–6]. These experimental findings have revived the interest for macroscopic biaxiality [7,8], and scientific debate, as is the case witnessed by the recent dispute [9,10] on what had started to be considered as a firm evidence of macroscopic biaxiality in thermotropic liquid crystals [11].

Financial support from the Royal Society of London through the Project *Biaxial liquid crystals: mathematical models and simulation* is gratefully acknowledged.

Address correspondence to Fulvio Bisi, Dipartimento di Matematica and CNISM, Università di Pavia, Via Ferrata 1, 27100 Pavia, Italy. E-mail: fulvio.bisi@unipv.it

The phase diagrams for biaxial nematics so far proposed can be reduced to two types, essentially. The first one shows invariably the same mean-field phase diagram, with a single triple point [12–17]. This can be obtained by using the well-accepted idea that macroscopic biaxiality results from anisotropic dispersion forces between biaxial molecules [1]; in addition to that, excluded-volume effects have also been studied, with no change in the result. In the dispersion model, each fluctuating dipole of a molecule interacts with all induced dipoles in another molecule. In general, a dipole of a real molecule always interacts with the corresponding dipole of another molecule, but it may not interact with the other dipoles, which resonate at different frequencies. Ideally, one could think of molecules composed of "independent" oscillators. The second type of phase diagram is more recent; in this case a mean-field model has been applied to molecules for which dispersion forces arise from two independent sources [18]. The phase diagram predicted is very different from the former, which wrongly appeared to be universal. In fact, the latter shows the onset of two tricritical points [19,20]. However, all models previously studied are peculiar cases of the general Straley quadrupolar interaction potential [12]; indeed, this potential has been studied both analytically, in the mean-field approximation [12,13,21], and computationally [22,23,16,15], mainly within the London dispersion forces approximation (see [24] and Sect. 5.1 of [25]). In consideration of that, it is interesting to investigate which variety of phase diagrams arises from Straley's general interaction. A partial answer has already been given by Longa *et al.* [26]: they showed that the tricritical point found in [18] extends as a line in the parameter space. We will show that the two tricritical points found in [19,20] are joined by this line so that the phase diagram presented in [18] describes in full generality the behavior of biaxial liquid crystals within the quadrupolar approximation.

In detail, we employed a mean-field model based on a particular version of Straley's potential going past the dispersion forces approximation. Physically, such model is built on the idea that different oscillators in a molecule can resonate only with their counterpart in the interacting molecule, instead of resonating with all, as implied in London dispersion forces approximation. This model, which was further studied in [20,19], revealed a new bifurcation scenario, which includes a tricritical point along the uniaxial-to-biaxial phase transition and the possibility of a direct, first-order isotropic-to-biaxial transition.

In particular, Straley's quadrupolar Hamiltonian for nematogenic biaxial molecules can be either *fully attractive* or *partly repulsive*. In both cases, Hamiltonians are globally attractive, and promote the

state where all molecules, depicted as blocks, lie parallel to one another, side by side. On the one hand, fully attractive Hamiltonians result from the superposition of attractive, purely dispersive interactions. On the other hand, partly repulsive Hamiltonians result from the superposition of both attractive, purely dispersive interactions and excluded-volume, repulsive interactions. It has recently been shown that the quadrupolar approximation of the excluded-volume interaction associated with a large class of biaxial molecules introduced by Mulder [27], the sphero-cuboids, is partly repulsive [28]. This class of molecules includes both Straley's blocks [12,14] and spheroplatelets [29,30] as special cases. For all sphero-cuboids, the repulsive component in the effective quadrupolar pair-potential is reminiscent of the parent hard-core interaction. It has been conjectured in [28] that the excluded-volume interaction of all biaxial molecules have a partly repulsive quadrupolar approximation.

In order to deal with partly repulsive Hamiltonians, we had to resort to a variational principle suited to a general class of Hamiltonians, as the approximate free energy computed may fail to attain its minimum at every stationary point. This can be done by applying a minimax principle to the mean-field approximation to the free energy [31].

By following this route, we have been able to show that the phase diagram previously obtained [28] is indeed universal, in the sense that other phase diagrams are qualitatively the same as that one, with the extension to a whole region of the molecular parameter space of both the direct first-order isotropic-to-biaxial transition and a tricritical point. Moreover, for all partly repulsive interactions, the phase diagram is qualitatively the same as the one predicted in the case of purely London dispersive interactions, with a single triple point marking a second-order isotropic-to-biaxial transition.

2. BIAXIAL INTERACTIONS

When molecules interact, their interaction Hamiltonian H reflects the molecular symmetry. By assuming, as customary for nematic liquid crystals, that the molecular distribution is homogeneous in space and isotropic in the intermolecular vector, for any given relative orientation, we reduce H to its orientational part. In particular, here we study the general quadrupolar orientational Hamiltonian put forward by Straley [12], phrased in the tensorial formalism of [18].

We describe the interacting molecules through two pairs of symmetric, traceless tensors, $(\mathbf{q}, \mathbf{b})$ and $(\mathbf{q}', \mathbf{b}')$. Both tensors $\mathbf{q}$ and $\mathbf{q}'$ are uniaxial around the unit molecular vectors $\boldsymbol{m}$ and $\boldsymbol{m}'$; both $\mathbf{b}$ and $\mathbf{b}'$, orthogonal to $\mathbf{q}$ and $\mathbf{q}'$, respectively, are purely biaxial. Explicit

representations of $\mathbf{q}$ and $\mathbf{b}$ are

$$\mathbf{q} := \boldsymbol{m} \otimes \boldsymbol{m} - \frac{1}{3}\mathbf{I}, \tag{1a}$$

$$\mathbf{b} := \boldsymbol{e} \otimes \boldsymbol{e} - \boldsymbol{e}_\perp \otimes \boldsymbol{e}_\perp, \tag{1b}$$

where $\mathbf{I}$ is the identity tensor, and the orthonormal basis $(\boldsymbol{e}, \boldsymbol{e}_\perp, \boldsymbol{m})$ is the eigenframe of any molecular susceptibility tensor, $\mathbf{q}$ and $\mathbf{b}$ representing the irreducible components of the anisotropic part of any such tensor. Similar representations apply to $\mathbf{q}'$ and $\mathbf{b}'$ in the eigenframe $(\boldsymbol{e}', \boldsymbol{e}'_\perp, \boldsymbol{m}')$ (Fig. 1). In terms of these tensors, H can be written as

$$H = -U\{\xi \mathbf{q} \cdot \mathbf{q}' + \gamma(\mathbf{q} \cdot \mathbf{b}' + \mathbf{b} \cdot \mathbf{q}') + \lambda \mathbf{b} \cdot \mathbf{b}'\}, \tag{2}$$

where $U > 0$ is a scaling energy, $\xi = \pm 1$, and γ, λ are dimensionless scalar parameters.

For $\xi = 1$, the Hamiltonian in (2) constitutes the natural extension to biaxial molecules of Maier and Saupe's interaction for cylindrically symmetric molecules [32]. A special instance of H is obtained by

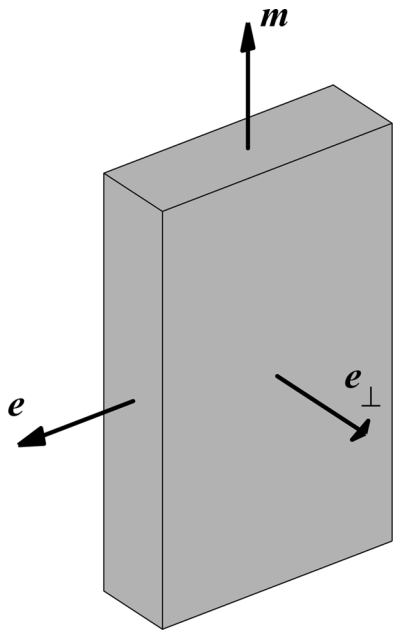

FIGURE 1 A pictorial representation of a biaxial molecule as a platelet with a major axis $\boldsymbol{m}$ and two minor axes, $\boldsymbol{e}$ and $\boldsymbol{e}_\perp$. These are the eigenvectors of any molecular polarizability tensor.

setting $\lambda = \gamma^2$:

$$H = -U(\mathbf{q} + \gamma\mathbf{b}) \cdot (\mathbf{q}' + \gamma\mathbf{b}'). \tag{3}$$

This case, which we call *purely dispersive*, was first considered by Freiser [1,2]: it represents a London interaction associated with the molecular susceptibility $\mathbf{a}_p := \mathbf{q} + \gamma\mathbf{b}$. Compared to this, the general interaction (2) represents the case where the different arms of the molecules resonate at different frequencies [18,33]. For short, we often call $\lambda = \gamma^2$ the *dispersion parabola*.

For $\xi = -1$, a repulsive interaction between the long molecular axes $\boldsymbol{m}$ and $\boldsymbol{m}'$ is contrasted by dispersion interactions that potentially favour the alignment of the perpendicular axes $\boldsymbol{e}, \boldsymbol{e}'$ and $\boldsymbol{e}_\perp,\ \boldsymbol{e}'_\perp$.

Equation (2) can also be phrased in terms of the inner products between corresponding unit vectors in the molecular eigenframes [34]:

$$H = -U\left\{-(\lambda + \frac{\xi}{3}) + (\xi - \lambda)(\boldsymbol{m}\cdot\boldsymbol{m}')^2 + 2(\lambda+\gamma)(\boldsymbol{e}_\perp\cdot\boldsymbol{e}'_\perp)^2 + 2(\lambda-\gamma)(\boldsymbol{e}\cdot\boldsymbol{e}')^2\right\}. \tag{4}$$

3. GROUND STATE STABILITY

The Hamiltonians H in (2) or (4) represent the matching tendency of a pair of interacting molecules, *i.e.*, the tendency they have to be oriented alike, side by side, one parallel to the other. In other words, we require that H attains its absolute minimum when the molecular vectors $(\boldsymbol{e}, \boldsymbol{e}_\perp, \boldsymbol{m})$ and $(\boldsymbol{e}', \boldsymbol{e}'_\perp, \boldsymbol{m}')$ orderly coincide or, which is the same, when $\mathbf{q} = \mathbf{q}'$ and $\mathbf{b} = \mathbf{b}'$. To ensure that this is the ground state of H, the parameters γ and λ must be appropriately restrained. These restrictions are different for the two different values of ξ.

To formalize the requirement we need to impose on the ground state of H, we can consider a pair $(\mathbf{q}', \mathbf{b}')$ as obtained from $(\mathbf{q}, \mathbf{b})$ via a rotation of an angle $\alpha \in [0, \pi]$ about a rotation axis characterized by a unit vector $\boldsymbol{w}$.

If we denote by ΔH the difference between H in (2) and the value it takes on its supposed ground state, we observe that a necessary condition for ΔH to be positive definite for all α and $\boldsymbol{w}$ is being so for small values of α and all $\boldsymbol{w}$. To express this local stability condition for H, we write the lowest approximation to ΔH for $\alpha \ll 1$, and denote it by δH.

It turns out [35] that δH is positive for all components of $\boldsymbol{w}$ provided that

$$\lambda > 0 \quad \text{and} \quad \xi - |2\gamma| + \lambda > 0. \tag{5}$$

δH can also be given the compact form

$$\delta H = \boldsymbol{k} \cdot \boldsymbol{\omega}, \tag{6}$$

where $\boldsymbol{\omega} = \alpha\boldsymbol{\omega}$ is the rotation vector and $\boldsymbol{k}$, which depends linearly on $\boldsymbol{\omega}$,

$$\boldsymbol{k} = \mathbf{M}\boldsymbol{\omega}, \tag{7}$$

is the corresponding *restoring torque*. In the molecular frame $(\boldsymbol{e}, \boldsymbol{e}_\perp, \boldsymbol{m})$, the tensor $\mathbf{M}$ in (7) is represented as

$$\mathbf{M} = (\xi + 2\gamma + \lambda)\boldsymbol{e} \otimes \boldsymbol{e} + (\xi - 2\gamma + \lambda)\boldsymbol{e}_\perp \otimes \boldsymbol{e}_\perp + 4\lambda \boldsymbol{m} \otimes \boldsymbol{m}. \tag{8}$$

For $\xi = 1$, $\mathbf{M}$ possesses two equal eigenvalues whenever one of the following equations is satisfied:

$$1 - 2\gamma - 3\lambda = 0, \quad 1 + 2\gamma - 3\lambda = 0, \quad \gamma = 0. \tag{9}$$

Correspondingly, $\mathbf{M}$ is uniaxial about $\boldsymbol{e}, \boldsymbol{e}_\perp$, or $\boldsymbol{m}$. Equations (9) determine three straight lines in the (γ, λ) plane (see Fig. 2), along which the distribution of restoring torques is uniaxial. We call them the *uniaxial-torque* lines. They all meet at the point $\mathsf{I} = \left(0, \frac{1}{3}\right)$: there,

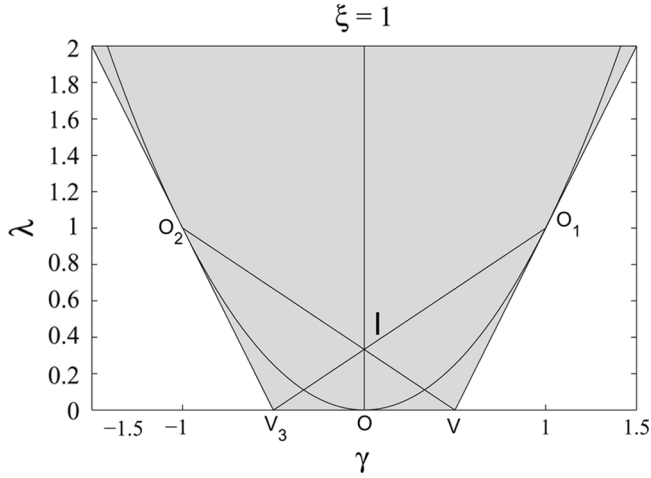

FIGURE 2 The domain of stability for the interaction Hamiltonian H (2) in the plane $\xi = 1$. The straight lines $\gamma = 0$ and $1 \pm 2\gamma - 3\lambda = 0$ embody the symmetries of H. The points O, O_1, and O_2 are conjugated. The points on the parabola $\lambda = \gamma^2$ represents the purely dispersive case (3).

M is isotropic, and $\boldsymbol{k}$ is thus aligned to $\boldsymbol{\omega}$. For $\xi = -1$, **M** is uniaxial (about $\boldsymbol{m}$) only for $\gamma = 0$.

The local stability analysis performed above for the ground state of H can easily be extended to the other critical points of H. It can be shown that H is stationary at the pairs $(\boldsymbol{e}, \boldsymbol{e}_\perp, \mathbf{m})$ and $(\boldsymbol{e}', \boldsymbol{e}'_\perp, \boldsymbol{m}')$ whenever

$$\begin{aligned}[(\xi - \lambda)(\boldsymbol{m} \cdot \boldsymbol{m}')\boldsymbol{m} \otimes \boldsymbol{m}' + 2(\lambda + \gamma)(\boldsymbol{e}_\perp \cdot \boldsymbol{e}'_\perp)\boldsymbol{e}_\perp \otimes \boldsymbol{e}'_\perp \\ + 2(\lambda - \gamma)(\boldsymbol{e} \cdot \boldsymbol{e}')\boldsymbol{e} \otimes \boldsymbol{e}'] \in Sym,\end{aligned} \tag{10}$$

where *Sym* is the subspace of all symmetric tensors. Clearly, (10) is satisfied for all molecular orientations with axes $(\boldsymbol{e}', \boldsymbol{e}'_\perp, \boldsymbol{m}')$ obtained by permutation of the axes $(\boldsymbol{e}, \boldsymbol{e}_\perp, \boldsymbol{m}')$: in all these configurations, each symmetry axis in one molecule is aligned to a symmetry axis in the other molecule, though not all equal axes are parallel to one another. We call these configurations *aligned*. One can prove that, for $\xi = 1$, minima and maxima of H can only occur at the aligned configurations. In addition to that, for $\xi = -1$, among all aligned configurations, H attains its maximum only when $\boldsymbol{m} = \boldsymbol{m}'$: all other configurations but the ground state are saddle points. We need not dwell any further on the analysis of H for $\xi = -1$, as it will be shown in the following section that this case can easily be recovered from the case $\xi = 1$ by an appropriate permutation of the molecular axes. In view of this, we conclude that the ground state is actually the global minimizer for H in the whole domain of stability.

4. PERMUTATION SYMMETRIES

Calling the molecular axes the way we have chosen is a matter of convention; we could agree to orient $\boldsymbol{e}$, $\boldsymbol{e}_\perp$, and $\boldsymbol{m}$ along the principal orientations of a molecular susceptibility tensor, respectively, in increasing order of the corresponding principal susceptibilities. Such a choice would unambiguously identify three orthogonal molecular axes, but none of these conventional choices in indeed necessary for the validity of our theory. As already remarked in [8], H represents physically the same system if the names of the molecular axes are swapped, provided that the scalar coefficients of the corresponding bilinear terms in either Eqs. (2) or (4) are accordingly exchanged.

There are three different transformations $(\xi, \gamma, \lambda) \mapsto (\xi_i^*, \gamma_i^*, \lambda_i^*)$, $i = 1, 2, 3$, characterized by which molecular axis is left unchanged. Without going into details, which can be obtained elsewhere [35] we can say the corresponding transformations for the molecular tensors

q and **b** read as

$$\mathbf{q}_1^* = -\frac{1}{2}(\mathbf{q}+\mathbf{b}), \quad \mathbf{b}_1^* = -\frac{1}{2}(3\mathbf{q}-\mathbf{b}), \tag{11a}$$

$$\mathbf{q}_2^* = -\frac{1}{2}(\mathbf{q}-\mathbf{b}), \quad \mathbf{b}_2^* = \frac{1}{2}(3\mathbf{q}+\mathbf{b}), \tag{11b}$$

$$\mathbf{q}_3^* = \mathbf{q}, \quad \mathbf{b}_3^* = -\mathbf{b}. \tag{11c}$$

These transformation reveal the same structure under composition as the permutation group P_3. They can be given a rather intuitive geometric interpretation in the copies of the (γ, λ) plane corresponding to $\xi = \pm 1$.

For $\xi = 1$, the lines $1 \mp 6\gamma + 9\lambda = 0$ intersect the domain of stability (5) along the segments PP_1 and $\mathsf{P}_3\mathsf{Q}$ in Figure 3. The co-ordinates of

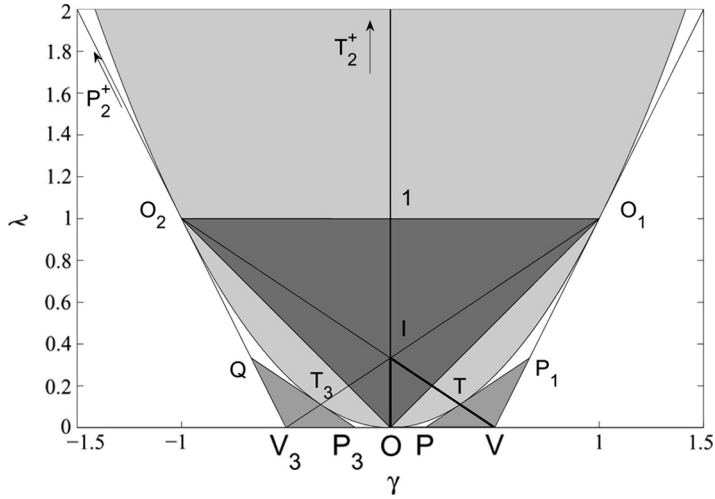

FIGURE 3 Conjugation chart. The domain of stability is divided in subregions mutually transformed in one another by permutation symmetries. The whole domain, on both planes $\xi = \pm 1$, is covered by the images of the essential triangle OIV in the plane $\xi = 1$. For each component of the essential triangle distinguished here by a different degree of grey, there are 5 equivalent copies, all in the plane $\xi = 1$, apart from two copies of PTV that lie in the plane $\xi = -1$.

the end-points of these segments are $\mathsf{P} = (\frac{1}{6}, 0)$, $\mathsf{P}_1 = (\frac{2}{3}, \frac{1}{3})$, and $\mathsf{P}_3 = (\frac{-1}{6}, 0)$, $\mathsf{Q} = (\frac{-2}{3}, \frac{1}{3})$.

Applying to the triangle OIV in Figure 3 a transformation in the permutation group generated by the three transformation rules, we can cover the whole domain of stability in both planes $\xi = \pm 1$. This allows restricting our consideration to such triangle, which we therefore call *essential*: all different choices of the model parameters, including those with $\xi = -1$, can easily be reproduced by an appropriate permutation of the molecular axes. Henceforth, our analysis of H will specifically apply to the essential triangle OIV in the plane $\xi = 1$.

5. HAMILTONIAN DIAGONALIZATION

The interaction energy (2) can always be written uniquely as a superposition of two quadratic terms like the one in (3):

$$H = -U(a^+ \mathbf{q}^+ \cdot \mathbf{q}^{+\prime} + a^- \mathbf{q}^- \cdot \mathbf{q}^{-\prime}) \tag{12}$$

with $\mathbf{q}^+$ and $\mathbf{q}^-$ orthogonal molecular tensors represented as

$$\mathbf{q}^\pm := \mathbf{q} + \gamma^\pm \mathbf{b} \tag{13}$$

For $\gamma \neq 0$,

$$\gamma^\pm = \frac{3\lambda - 1 \pm \sqrt{(3\lambda - 1)^2 + 12\gamma^2}}{6\gamma}, \quad a^+ = \frac{\gamma^- - \gamma}{\gamma^- - \gamma^+}, \quad \text{and} \quad a^- = \frac{\gamma - \gamma^+}{\gamma^- - \gamma^+}. \tag{14}$$

For $\gamma = 0$, $\mathbf{q}^+ = \mathbf{q}$ and $\mathbf{q}^- = \mathbf{b}$, while $a^+ = 1$ and $a^- = \lambda$. We notice that the values $\gamma^\pm$ in (14) have always opposite sign. Moreover, whenever $\lambda > \gamma^2$ both $a^\pm$ are positive, and so H is decomposed by (12) into two London *attractors*. On the other hand, whenever $\lambda < \gamma^2$ one amplitude $a^\pm$ is positive and the other is negative, and so H is decomposed by (12) into a London attractor and a London *repulsor* [31]. The Hamiltonian is said *fully attractive* in the former case and *party repulsive* in the latter. If $\lambda = \gamma^2$,

$$\gamma^+ = \gamma, \quad \gamma^- = -\frac{1}{3\gamma} \quad \text{and} \quad a^+ = 1, \quad a^- = 0, \tag{15}$$

and (12) reduces to (13).

This decomposition of H can be given a telling geometric interpretation (see Fig. 4). For a given point (γ, λ) representing H in (2), the corresponding points $(\gamma^\pm, \lambda^\pm)$ are the intersections of the parabola $\lambda = \gamma^2$ with the straight line through the points (γ, λ) and $\mathsf{I} = (0, \frac{1}{3})$. Thus,

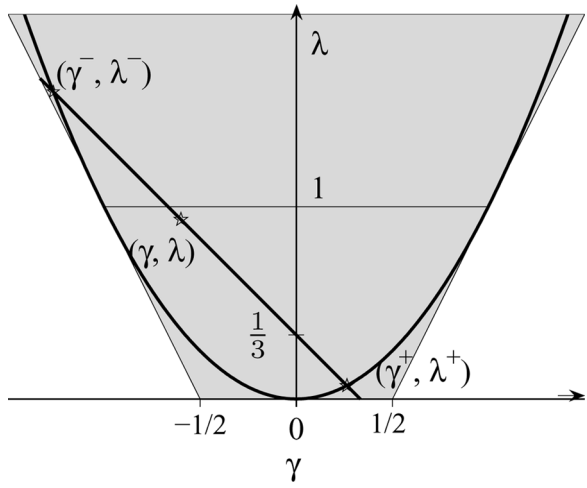

FIGURE 4 The shaded fan in the (γ, λ) plane represents the region where H in (2) attains its minimum when $(\mathbf{q}', \mathbf{b}') = (\mathbf{q}, \mathbf{b})$. The points $(\gamma^{\pm}, \lambda^{\pm})$ on the dispersion parabola $\lambda = \gamma^2$ represent the quadratic decomposition of an interaction described by (γ, λ) (12).

all points (γ, λ) on this line are associated with the same roots $\gamma^{\pm}$, but with different amplitudes $a^{\pm}$.

6. MINIMAX PRINCIPLE

The standard strategy to find the stable phases of a system undergoing an ordering transition is to minimize the mean-field approximation F_0 to the free energy F of the system. There exist examples showing that the presence of repulsive terms in the Hamiltonian can make this strategy fail [37]. For systems described by discrete state variables, a remedy to this failure is known to be the minimax principle first proposed by Bogolubov Jr. in the study of a model problem in superconductivity and later extended to more general spin systems [38,39]. Recently, such principle has been proposed for systems described by continuous state variables, as are biaxial nematic liquid crystals [31].

In the following, we will restrict all considerations to our model. In general, two independent order tensors are needed to describe all possible condensed phases predicted by the interaction Hamiltonian H in (2). They can be defined as

$$\mathbf{Q} := \langle \mathbf{q} \rangle, \quad \mathbf{B} := \langle \mathbf{b} \rangle, \tag{16}$$

where $\langle\cdot\rangle$ denotes the ensemble average relative to the single-particle distribution function.

Under the assumption that the macroscopic tensors $\mathbf{Q}$ and $\mathbf{B}$ share the same eigenframe, which is sensibly assumed in the absence of external fields, four scalar order parameters, S, T, S', T', suffice to represent them:

$$\mathbf{Q} = S\left(\boldsymbol{e}_z \otimes \boldsymbol{e}_z - \frac{1}{3}\mathbf{I}\right) + T(\boldsymbol{e}_x \otimes \boldsymbol{e}_x - \boldsymbol{e}_y \otimes \boldsymbol{e}_y), \tag{17a}$$

$$\mathbf{B} = S'\left(\boldsymbol{e}_z \otimes \boldsymbol{e}_z - \frac{1}{3}\mathbf{I}\right) + T'(\boldsymbol{e}_x \otimes \boldsymbol{e}_x - \boldsymbol{e}_y \otimes \boldsymbol{e}_y), \tag{17b}$$

S and S' are uniaxial order parameters. If both T and T' vanish, we say that $\mathbf{Q}$ and $\mathbf{B}$ represent a uniaxial phase: the intrinsic molecular biaxiality is not collectively revealed. When either T or T' is different from zero, we say that the phase is biaxial and two different origins can be identified for this collective behaviour: in the distribution of the molecular long axes, if $T \neq 0$, or in the intrinsic molecular biaxiality, if $T' \neq 0$.

Equivalently, in view of the decomposition used in (12), we could resort to the averages of the molecular tensors (13). We can thus describe the condensed phases in terms of two new tensors, which can be defined analogously:

$$\mathbf{Q}^- = \langle \mathbf{q}^- \rangle = S^-\left(\boldsymbol{e}_z \otimes \boldsymbol{e}_z - \frac{1}{3}\mathbf{I}\right) + T^-(\boldsymbol{e}_x \otimes \boldsymbol{e}_x - \boldsymbol{e}_y \otimes \boldsymbol{e}_y), \tag{18a}$$

$$\mathbf{Q}^+ = \langle \mathbf{q}^+ \rangle = S^+\left(\boldsymbol{e}_z \otimes \boldsymbol{e}_z - \frac{1}{3}\mathbf{I}\right) + T^+(\boldsymbol{e}_x \otimes \boldsymbol{e}_x - \boldsymbol{e}_y \otimes \boldsymbol{e}_y). \tag{18b}$$

Therefore, the free energy F_0 of the condensed phases is a function of a set of four order parameters (S^+, T^+, S^-, T^-). For partly repulsive Hamiltonians, the stable condensed phases must be a local maximum in $\mathbf{Q}^-$, and a local minimum in $\mathbf{Q}^+$, the minimax principle boils down to the *third eigenvalue criterion*. In other words, a state that can be classified in the mean field approximation as locally stable must have the hessian form of F_0 with respect to the four variables characterized by two stable normal modes and two unstable ones, *i.e.*, once the eigenvalues of the hessian matrix are sorted in ascending order, the third eigenvalue must be positive.

7. PHASE SEQUENCES

In this section, with the aid of the minimax principle detailed in Sec. 6, we determine the sequence in temperature of all stable phases described by the mean-field free energy F_0 associated with the interaction Hamiltonian in Eq. (12).

We use the symmetries induced by the permutations of the molecular axes introduced by Longa *et al.* [26] and described in Section 4. For example, the point O, O_1, and O_2 in Figure 5 all represent the same interaction energy of equivalent uniaxial molecules with symmetry axes along the molecular frame $(\boldsymbol{e}, \boldsymbol{e}_\perp, \boldsymbol{m})$. Similarly, the range of uniaxial stability about $\boldsymbol{m}$, which in Figure 5 is represented by a triangle in the plane $\lambda < 0$, is mapped into the infinite triangles defined by $\lambda > 0$ and $\lambda - |2\gamma| + 1 < 0$, when $\boldsymbol{m}$ is replaced by either $\boldsymbol{e}$ or $\boldsymbol{e}_\perp$. As

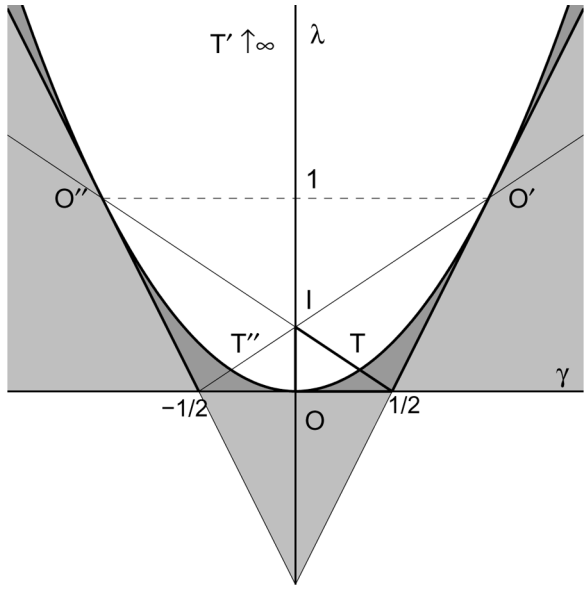

FIGURE 5 The region above the dispersion parabola $\lambda = \gamma^2$ represents fully attractive Hamiltonians, while the region below this parabola represents partly repulsive Hamiltonians. The grey triangle in the half-plane $\lambda < 0$ is the region to be added to the fan, if only the stability of molecules around their long axes is required in the ground state. The two other grey regions are conjugated to this triangle via the permutations symmetries of H. O, O′, and O″ represent purely uniaxial interactions. T, T, and T″ represent purely biaxial interactions. T′ is the point at infinity of the parabola. The lines OT′, O′T″, and O″T represent the permutation symmetries of H: they all meet at the point I.

shown in [26], all inequivalent H's are represented by points in the *essential* triangle in Figure 6 extracted from Figure 5. All the points conjugated under one of these symmetries should give rise to the same physical behaviour, provided the temperature is appropriately rescaled whenever the molecular axis $\boldsymbol{m}$ is not involved in the permutation.

The sides of the essential triangle within the fan-region are self-conjugated under permutation symmetries. For each side there is a transformation of the microscopic state that leaves the interaction energy invariant with no associated change in the temperature scale. Thus, a new property arises. Any macroscopic quadrupolar observable $\mathbf{A}$ can be written as a linear superposition of the ensemble averages $\mathbf{Q}$ and $\mathbf{B}$ of $\mathbf{q}$ and $\mathbf{b}$: $\mathbf{A} = \alpha\mathbf{Q} + \beta\mathbf{B}$. The corresponding measurable physical quantities are expressed in terms of their spectra. By imposing the invariance of the spectra under the symmetry transformations that make the Hamiltonian H self-conjugated, we find new constraints on the admissible order tensors $\mathbf{Q}$ and $\mathbf{B}$. The simplest case occurs for $\gamma = 0$, where the exchange of $\boldsymbol{e}$ and $\boldsymbol{e}_\perp$ does not change H. By requiring that for $\gamma = 0$ the algebraic invariants of $\mathbf{A}^* = \alpha\mathbf{Q} - \beta\mathbf{B}$ be the same as the algebraic invariants of $\mathbf{A}$ for all α and β, we arrive at [35]

$$\mathrm{tr}(\mathbf{QB}) = \mathbf{Q} \cdot \mathbf{B} = 0, \quad \mathrm{tr}(\mathbf{Q}^2\mathbf{B}) = 0, \quad \mathrm{tr}(\mathbf{B}^3) = 0. \tag{19}$$

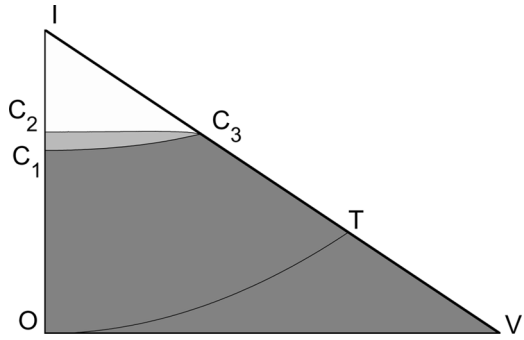

FIGURE 6 The essential triangle, delimited by thick lines of Figure 5. The base OV represents Hamiltonians that give rise only to the isotropic-to-uniaxial transition. $\mathsf{C}_1\mathsf{C}_3$ is a tricritical line: the corresponding Hamiltonians produce a phase diagram with a tricritical point along the uniaxial-to-biaxial transition. $\mathsf{C}_2\mathsf{C}_3$ is a triple line: the corresponding Hamiltonians produce a phase diagram with a single direct isotropic-to-biaxial transition, where the isotropic, uniaxial, and biaxial phases are in equilibrium. T is the Landau triple point on the dispersion parabola. $\mathsf{C}_3\mathsf{V}$ is a line of triple points. There, a biaxial phase continuously branches off the isotropic phase.

Here, $\mathbf{Q}$ and $\mathbf{B}$ are the traceless order tensors defined in (16) [12,18]. As a consequence of constraints (19), $T = S' = 0$, and so for $\gamma = 0$ all condensed phases can be described by two scalar order parameters, S and T'. Since $\mathbf{Q}$ and $\mathbf{B}$ are orthogonal, one could be tempted to describe the ordered phase by a single tensorial order parameter. This would be misleading because the biaxialities of $\mathbf{Q}$ and $\mathbf{B}$ have different molecular origins: the quadrupolar interactions between the $\mathbf{q}$'s and the $\mathbf{b}$'s are assumed to be independent, and so they cannot be expressed by the interactions of a combined molecular tensor. The constraints in (19) for $\gamma = 0$ have their counterpart on the self-conjugated lines $1 - 3\lambda \pm 2\gamma = 0$, where the phase ordering is again described by two scalar order parameters, conjugated to S and T' [35]: in particular, along the side IV of the essential triangle

$$3\mathrm{tr}(\mathbf{Q}^2) - \mathrm{tr}(\mathbf{B}^2) - 2\mathrm{tr}(\mathbf{QB}) = 0, \tag{20a}$$

$$\mathrm{tr}\,\mathbf{B}^3 - 9\mathrm{tr}\,\mathbf{Q}^2\mathbf{B} = 0, \tag{20b}$$

$$3\mathrm{tr}\,\mathbf{Q}^3 + 4\mathrm{tr}\,\mathbf{Q}^2\mathbf{B} + \mathrm{tr}\,\mathbf{QB}^2 = 0. \tag{20c}$$

Combining condition (20a) with (19), we find that the phase sequence for the intersection I of the three self-conjugated lines is described by a single scalar order parameter, since $S = T'$ for all temperatures. Thus, symmetry requires that if there is any ordering transition at I, this must be a direct first-order isotropic-to-biaxial transition. Had we united S and T' in the same order tensor, we would now arrive at the conclusion that the ordered phase is uniaxial, in contradiction with the result of [18]. Moreover, at the point I the degree of biaxiality of any macroscopic quadrupolar observable is predicted to be independent of the temperature.

We now discuss the sequences of ordered phases for choices of (γ, λ) inside the essential triangle, for both fully attractive and partly repulsive Hamiltonians. In the mean-field approximation, H is replaced by

$$H_0 = -U\left\{a^+\left(\mathbf{q}^+ - \frac{1}{2}\mathbf{Q}^+\right)\cdot\mathbf{Q}^+ + a^-\left(\mathbf{q}^- - \frac{1}{2}\mathbf{Q}^-\right)\cdot\mathbf{Q}^-\right\},$$

where $\mathbf{Q}^+$ and $\mathbf{Q}^-$ are the order tensors defined as in (13).

We showed in [31] that for quadratic Hamiltonians the minimax and the maximin principles provide equivalent strategies to find the

best approximation to the minimizer of the free energy F associated with the two-particle Hamiltonian H. For fully attractive Hamiltonians ($a^{\pm} > 0$), we minimize F_0 in its four scalar variables. For partly repulsive Hamiltonians ($a^{+} > 0$, $a^{-} < 0$), we seek the stationary points of F_0 with minimal energy: these are saddle points of F_0, maxima in (S^{-}, T^{-}) and minima in (S^{+}, T^{+}).

We performed a numerical bifurcation and continuation analysis of the stationary points of F_0 along straight lines through the vertex $\mathsf{I} = (0, \frac{1}{3})$ of the essential triangle (details are given elsewhere [35,40]). Along the line $\gamma = 0$, the phase diagram is already known [18] and is governed, as expected, only by two scalar order parameters: it features a tricritical point $\mathsf{C}_1 \simeq (0, 0.20)$ for the uniaxial-to-biaxial transition and a triple point $\mathsf{C}_2 \simeq (0, 0.22)$ between isotropic, uniaxial and biaxial phases. It follows from [20,19] and the permutation symmetries that along the side IT of the essential triangle there is a tricritical point at $\mathsf{C}_3 = \left(\frac{5}{29}, \frac{19}{87}\right)$ for the isotropic-to-biaxial transition. Within the essential triangle we find, as in [26], a line of tricritical points that joins C_1 and C_3. In addition, there is a line of triple points starting from C_2 and also ending at C_3, where both this line and the tricritical line appear on close inspection to be tangent to the side IT (see Fig. 6). Along the segment IC_3 the system undergoes a single first order isotropic-to-biaxial transition [19]. All points of the segment $\mathsf{C}_3\mathsf{T}$ are triple points, but those of the segment IC_3 are not: this corrects the prediction in [26], according to which the whole side IV should consist of triple points.

It should be noted that for partly repulsive Hamiltonians we always find the same phase diagram of [12], which coincides with the one obtained for a single London attractor on the dispersion parabola [13]. The base OV of the essential triangle represents Hamiltonians H for which there exists a single first order isotropic-to-uniaxial transition. This confirms the prediction made in [23] by early Monte Carlo simulations of biaxial systems.

We also explored the segment TV by enforcing constraints (20) on the order tensors $\mathbf{Q}$ and $\mathbf{B}$. Seen in this constrained manifold, TV exhibits only triple points, that is, the corresponding Hamiltonians describe a system that undergoes the isotropic-to-biaxial transition at a single point in the phase diagram, where three phases coexist in equilibrium: isotropic, uniaxial, and biaxial [35].

The phase diagram that used to be considered universal previously extends inside the triangle only up to the tricritical line $\mathsf{C}_1\mathsf{C}_3$. It is characterized by a first-order isotropic-to-uniaxial nematic transition followed, at a lower temperature, by a second-order uniaxial-to-biaxial transition. Between the lines $\mathsf{C}_1\mathsf{C}_3$ and $\mathsf{C}_2\mathsf{C}_3$, we observe the same

sequence of phases, but with simple first-order transitions. In the corner of the triangle above the line $\mathsf{C}_2\mathsf{C}_3$ there is only a direct first-order transition between the isotropic and biaxial phases.

A convenient way of representing the universal phase diagram, featuring all the phase sequences described here, is restricting the molecular parameter space to the boundary OITV of the essential triangle. We call λ^* the arc-length along this folded line. Formally, the interaction parameter λ^* is the arc-length along the upper border OIV of the essential triangle:

$$\lambda^* := \begin{cases} \lambda \in [0, \frac{1}{3}] & \text{if } \gamma = 0 \\ \frac{1}{3}(1 + \sqrt{13}\gamma) & \text{if } \gamma = \frac{1}{2}(1 - 3\lambda) \in [0, \frac{1}{2}] \end{cases} \tag{21}$$

The transition temperature $\frac{1}{\beta^*}$ is scaled to the condensation energy U^* of the attractive well of H in (12): k_B is the Boltzman constant, and t

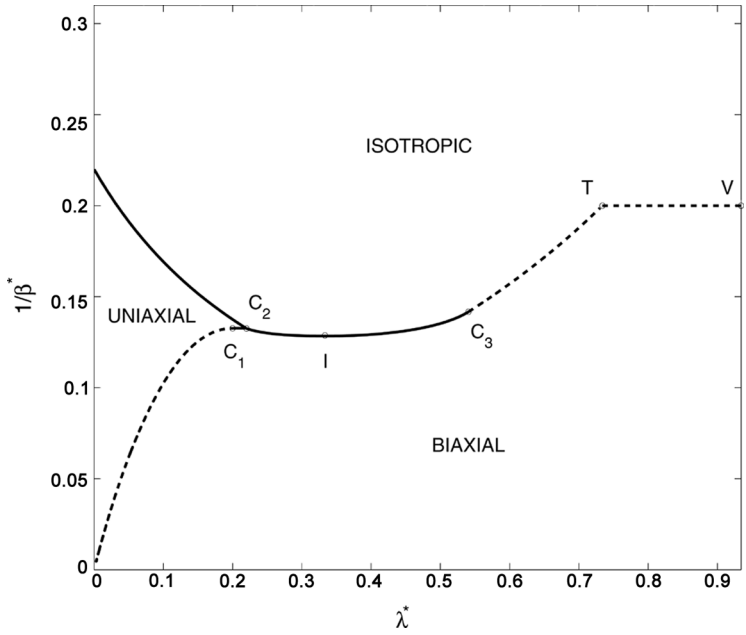

FIGURE 7 Phase diagram along the edges OI and IV of the essential triangle. The scaled transition temperature $1/\beta^*$ is plotted as a function of the interaction parameter λ^* defined in (21). C_1 and C_3 are tricritical points already known from [18–20]. C_2 is a triple point, where isotropic, uniaxial, and biaxial phases coexist in equilibrium. Solid lines represent first-order transitions; broken lines represent second-order transitions [35].

is the absolute temperature

$$\frac{1}{\beta^*} := \frac{k_B t}{U^*}, \quad \text{where } U^* = \begin{cases} \frac{2}{3}U(1+3\lambda) & \text{if } \lambda \geq \gamma^2 \\ U(1-\lambda) & \text{if } \gamma = \frac{1}{2}(1-3\lambda) \in \left[\frac{1}{3}, \frac{1}{2}\right] \end{cases} \tag{22}$$

As customary, in Figure 7 broken lines denote second-order transitions and solid lines first-order transitions. In particular, we find that on the segment $\mathsf{C}_3\mathsf{V}$ of all triple points for the fully attractive interactions the maximum transition temperature occurs on TV.

Straley [12] put forward the most general quadrupolar molecular interaction, and yet the phase diagram derived from his specific excluded-volume computation did not reveal any of the features discovered here. The reason for this is simple: Straley's excluded-volume interaction Hamiltonian can only be mapped into the partly repulsive region; the associated amplitude U in (12) vanishes along the London dispersion parabola (see Fig. 5) [28].

8. DISCUSSION

For experimentalists to observe a stable thermotropic biaxial phase it is essential to choose molecules with fully attractive interactions, which in principle would give rise to a direct isotropic-to-biaxial transition. We know from our study that, to attain the highest transition temperature with attractive interactions, one should choose molecules that interact through the Hamiltonian described by one of the three fully biaxial London points T, T', T'' (see Fig. 5).

This strategy has been quite fruitful. Liquid crystal chemists know very well how to synthetize uniaxial molecules giving rise to large nematic temperature ranges. Making V-shaped molecules using two symmetric identical rod-like arms has been successfully proposed to create a biaxial nematic phase [3,4,41]. A more detailed discussion on this issue can be found in [31].

Another interesting realization of biaxial mesogenic molecules are the tetrapodes employed in [6]. With the aid of two different compounds, experimental evidence of the tricritical point along the uniaxial-to-biaxial transition line was found. This appears to us as the first experimental validation of the universal character of the phase diagram predicted here. It follows from the phase diagram observed in [6] that one of the points representing the molecular interaction energy of the two compounds must lie inside the region $\mathsf{C}_1\mathsf{C}_2\mathsf{C}_3$ in Figure 6, while the other lies below it. It is plausible that in these

tetrapodes the biaxial character is due to the X-shaped central element with high polarizability.

Our model allows making new predictions for systems composed of independent London oscillators. For instance, since the superposition of two independent uniaxial oscillators of equal strength represented by the points O and O′ results in a state described by a point along IT not far from T, another strategy to engineer a nematogenic molecule with biaxial thermotropic phases would be to join at right angles two uniaxial arms, mutually orthogonal and independent.

9. CONCLUSIONS

We made a systematic analysis of the phases created by the most general quadrupolar Hamiltonian for anisotropic molecular interactions. Such a Hamiltonian can be classified as either fully attractive or partly repulsive. To find the best mean-field approximation to the free energy of the system, extension of Bogolubov's minimax principle to continuous state variables is needed. We applied this method to find the sequence of equilibrium phases in the essential region of the parameter space, for both fully attractive and partly repulsive interactions.

For all attractive interactions, the phase diagram is qualitatively the same as the one found in [18], with the extension to a whole region of the molecular parameter space of both the direct first-order isotropic-to-biaxial transition and a tricritical point. For all partly repulsive interactions, the phase diagram is qualitatively the same as the one predicted in the case of purely London dispersive interactions, with a single triple point marking a second-order isotropic-to-biaxial transition.

Although Straley proposed the most general quadrupolar molecular Hamiltonian adopted here, it turns out that his excluded-volume model covers only the partly repulsive case. The fully attractive case corresponds physically to pure dispersion forces interactions in the London and McLachlan approximations [25].

This explains why any simulation based on interactions with one London attractor and one London repulsor represented by a quadrupolar Straley's interaction must give qualitatively the same phase diagram with a single triple point, as the one obtained along the dispersion parabola. This led modelists to believe that this phase diagram is universal. In contrast with that, we showed that the most general fully attractive Straley's interaction gives rise to a phase diagram with both a tricritical and a triple point. This phase diagram includes the one obtained along the dispersion parabola as a special case, and so it is this one that must be regarded as universal.

Our predictions are in consistent with those made for both purely attractive and partly repulsive interactions of V-shaped mesogenic molecules. The observation of the tricritical point made with the tetrapodal molecules in [6] gives a first validation of the universal character of the phase diagram predicted here.

REFERENCES

[1] Freiser, M. J. (1970). *Phys. Rev. Lett.*, *24*, 1041.
[2] Freiser, M. J. (1971). *Mol. Cryst. Liq. Cryst.*, *14*, 165.
[3] Madsen, L. A., Dingemans, T. J., Nakata, M., & Samulski, E. T. (2004). *Phys. Rev. Lett.*, *92*, 145505.
[4] Acharya, B. R., Primak, A., & Kumar, S. (2004). *Phys. Rev. Lett.*, *92*, 145506.
[5] Severing, K. & Saalwächter, K. (2004). *Phys. Rev. Lett.*, *92*, 125501.
[6] Merkel, K., Kocot, A., Vij, J. K., Korlacki, R., Mehl, G. H., & Meyer, T. (2004). *Phys. Rev. Lett.*, *93*, 237801.
[7] Luckhurst, G. R. (2004). *Nature*, *430*, 413.
[8] Luckhurst, G. R. (2005). *Angew. Chem. Int. Ed.*, *44*, 2834.
[9] Galerne, Y. (2006). *Phys. Rev. Lett.*, *96*, 219803.
[10] Madsen, L. A., Dingemans, T. J., Nakata, M., & Samulski, E. T. (2006). *Phys. Rev. Lett.*, *96*, 219804.
[11] Madsen, L. A., Dingemans, T. J., Nakata, M., & Samulski, E. T. (2004). *Phys. Rev. Lett.*, *92*, 145505.
[12] Straley, J. P. (1974). *Phys. Rev. A*, *10*, 1881.
[13] Boccara, N., Mejdani, R., & De Seze, L. (1976). *J. de Phys. (Paris)*, *38*, 149.
[14] Mulder, B. (1989). *Phys. Rev. A*, *39*, 360.
[15] Biscarini, F., Chiccoli, C., Pasini, P., Semeria, F., & Zannoni, C. (1995). *Phys. Rev. Lett.*, *75*, 1803.
[16] Teixeira, P. I. C., Masters, A. J., & Mulder, B. M. (1998). *Mol. Cryst. Liq. Cryst.*, *323*, 167.
[17] Bates, M. A. & Luckhurst, G. R. (2005). *Phys. Rev. E*, *72*, 051702.
[18] Sonnet, A. M., Virga, E. G., & Durand, G. E. (2003). *Phys. Rev. E*, *67*, 061701.
[19] De Matteis, G., Romano, S., & Virga, E. G. (2005). *Phys. Rev. E*, *72*, 041706.
[20] De Matteis, G. & Virga, E. G. (2005). *Phys. Rev. E*, *71*, 061703.
[21] Ferrarini, A., Nordio, P. L., Spolaore, E., & Luckhurst, G. R. (1995). *J. Chem. Soc. Faraday Trans.*, *91*, 3177.
[22] Luckhurst, G. R., Zannoni, C., Nordio, P. L., & Segre, U. (1975). *Mol. Phys.*, *30*, 1345.
[23] Luckhurst, G. R. & Romano, S. (1980). *Mol. Phys.*, *40*, 129.
[24] London, F. (1937). *Trans. Faraday Soc.*, *33*, 8.
[25] Israelachvili, J. N. (1992). *Intermolecular and Surface Forces*, Academic Press: London.
[26] Longa, L., Grzybowski, P., Romano, S., & Virga, E. G. (2005). *Phys. Rev. E*, *71*, 051714.
[27] Mulder, B. M. (2005). *Mol. Phys.*, *103*, 1411.
[28] Rosso, R. & Virga, E. G. (2006). *Phys. Rev. E*, *74*, 0021712.
[29] Mulder, B. M. (1986). *Liq. Cryst.*, *1*, 539.
[30] Taylor, M. P. (1991). *Liq. Cryst.*, *9*, 141.
[31] Bisi, F., Virga, E. G., Gartland, E. C. Jr., De Matteis, G., Sonnet, A. M., & Durand, G. E. (2006). *Phys. Rev. E*, *73*, 051709.

[32] Maier, W. & Saupe, A. Z. Naturforsch. 14a, 882 (1959). Translated into English in Sluckin, T. J. Dunmur, D., & Stegemeyer, H. *Crystals that Flow*, pp. 381-385 (Taylor and Francis, London, 2004).
[33] Bergersen, B., Palffy-Muhoray, P., & Dunmur, D. A. (1988). *Liq. Cryst.*, *3*, 347.
[34] Romano, S. (2004). *Physica A*, *337*, 505.
[35] De Matteis, G., Bisi, F., & Virga, E. G. (2007). *Cont. Mech. Thermodyn.*, *19*, 1.
[36] Bergersen, B. & Palffy-Muhoray, P. (1988). *Liq. Cryst.*, *3*, 347.
[37] Osipov, M. A. & Shumovskii, A. S. (1981). *Teor. Mat. Fiz.*, *46*, 125; *Theor. Math. Phys.*, *46*, 83.
[38] Bogolubov, N. N. Jr. (1972). *A Method for Studying Model Hamiltonians*, Perg-amon Press: Oxford.
[39] Bogolubov, N. N. Jr., Sadovnikov, B. I., & Shumosky, A. S. (1994). *Mathematical Methods of Statistical Mechanics of Model Systems*, CRC Press: Boca Raton.
[40] Bisi, F., Romano, S., & Virga, E. G. (2007). *Phys. Rev. E*, *75*, 041705.
[41] Luckhurst, G. R. (2007). *Thin Solid Films*, *393*, 40.